

STUDY ON INTEGRATED RADAR-COMMUNICATION SIGNAL OF **OFDM-LFM** BASED ON FRFT

Kangrun Chen¹, Yang Liu¹, Wei Zhang¹

¹Research Institute of Electronic Science and Technology University of Electronic Science and Technology of China, Chengdu, China
chenkrun@163.com

Keywords: Integrated Radar-Communication, Fractional Fourier Transform, Orthogonal Frequency Division Multiplexing, Linear Frequency Modulation, Ambiguity Function, Range Resolution, **Bit Error Rate**, **BER**

Abstract

① LFM: 数据传输速率低;
② OFDM: 复杂, 破坏正交性.

① In view of the defects that low data transmission rate in integrated radar-communication system based on Linear Frequency Modulation (LFM), and ② integrated radar-communication system based on Orthogonal Frequency Division Multiplexing (OFDM) is sensitive to frequency shift, its orthogonality of subcarriers is also easily broken. For those problems, this paper presents a novel integrated radar-communication signal of OFDM-LFM, which uses orthogonal LFM signals as subcarriers and uses Fractional Fourier Transform (FRFT) as modulation and demodulation method, making a thorough analysis on spectrum distribution and factors on radar ambiguity function (AF) of integrated radar-communication signal respectively. It also takes a further research on the communication and radar performance of integrated radar-communication signal. Theoretical analysis and simulation results show that OFDM-LFM integrated signal based on FRFT achieves a great range resolution and low bit error rate (BER) compared with the traditional OFDM integrated signal in frequency selective fading condition. Moreover, it can meet the requirement of transmitting a large number of data in a short time.

1 Introduction

With the development of electronic communication and computer network technology, the traditional radar system with simple detection performance has been unable to meet every demand in the complicated environment, which makes multifunctional radar system become a trend in the future. Now it is a research hotspot to employ radar system for high data rate, long distance, reliable communication by making use of its wide bandwidth, high power and directing property [1].

Over the last two decades, many schemes have been proposed to deal with the key issue of sharing signal design of radar-communication. Opposite-slope LFM waveforms are used for radar and communication pulses, up-chirp LFM and down-chirp LFM represent “1” or “0” in binary data stream respectively [2]. Following the foundation of [2], a proposal of integrated radar-communication scheme

is presented based on the same chirp rate and different initial frequency of LFM, it can transmit multi-binary information in a single LFM signal through making use of FRFT [3]. However, both approaches cannot meet the demand of transmitting a large number of data, because their communication symbol rate corresponds to chirp rate only, which is typically orders of magnitude lower than the communication symbol rate that obtained by a real communication system with the same bandwidth. In recent years, another waveform of OFDM has been introduced to implement the integration of radar and communication due to its advantages of high spectral efficiency and robustness against fading and multipath propagation effect. A feasibility analysis and discussion on waveform design includes some considerations on system parameters are in [4], and a further research on target detection technology based on OFDM integrated radar-communication system is studied in [5]. Unfortunately, integration of radar and communication system based on OFDM is sensitive to frequency deviation, and its orthogonality of subcarriers is easily broken, leading to a severe inter-carrier interference (ICI).

In view of the above questions, this paper combines LFM with OFDM and makes an improvement, proposing a integrated radar-communication signal of OFDM-LFM, which uses orthogonal LFM signal as subcarrier and uses FRFT as modulation and demodulation method. Since LFM subcarrier has a large Doppler tolerance and cannot be faded by deep frequency selective fading channel comparing to sinusoidal subcarrier, thus, this approach not only can improve radar range resolution and spectral efficiency, but also transmit information reliably with its strong abilities to avoid Doppler Effect.

The rest of paper is organized as follow ① Section II introduces the OFDM-LFM waveform about mathematical expression, modulation/demodulation method, frequency spectrum of waveform ② Section III derives its ambiguity function ③ Simulation result and analysis are described in Section IV ④ Section V shows the final conclusions.

2 An OFDM-LFM Waveform

2.1 Mathematical Expression

Refer to OFDM [5], the complex envelope of OFDM-LFM baseband signal can be represented as

$$s(t) = \sum_{m=0}^{M-1} \sum_{n=0}^{N-1} a_{n,m} \phi_n(t - mT) \quad (1)$$

with M being the number of symbols modulated on each subcarrier, N being the number of subcarriers, $a_{n,m}$ representing the m^{th} symbol modulated on the n^{th} subcarrier, T being the OFDM-LFM symbol period, and $\phi_n(t)$ denoting the n^{th} orthogonal LFM subcarrier

$$\phi_n(t) = \exp(j2\pi f_n t + j\pi \mu t^2) \text{rect}(t/T) \quad (2)$$

where μ represents the chirp rate, f_n being the individual subcarrier initial frequency

$$f_n = n \cdot \Delta f \quad (3)$$

LFM subcarrier bands of transmitted signal are overlapped in every symbol, these subcarriers are orthogonal when

$$\Delta f = k \cdot (1/T) \quad (4)$$

where k is integer, Δf represents the subcarrier frequency interval. With the choice, we can obtain the total bandwidth of OFDM-LFM consists of the bandwidth of LFM subcarrier and subcarrier frequency interval

$$B = B_s + (N-1) \cdot \Delta f \quad (5)$$

where B_s is the bandwidth of each LFM subcarrier. This paper choose B_s equal to Δf , for dealing with side-lobe of synthesized output [6].

2.2 Modulation/Demodulation Method

OFDM-LFM waveform is a chirp-like signal, not suitable to adopt traditional Fourier transform as its modulation and demodulation method. The fractional Fourier transform, as a generalization of Fourier transform, is an appropriate method for processing chirp-like signals or signals passing through the linear time-varying system.

The FRFT of signal $x(t)$ is represented as [7]

$$X_p = \{F^p[x(t)]\}(u) = \int_{-\infty}^{+\infty} x(t) K_p(t, u) dt \quad (6)$$

where p is the order of FRFT, u is fractional Fourier domain, $\alpha = p\pi/2$ is the angle of time-frequency axis, and $K_p(u, t)$ represents the kernel of FRFT

$$K_p(u, t) = \begin{cases} A_\alpha \exp[j\pi(t^2 \cot \alpha - 2tucsc \alpha + u^2 \cot \alpha)] & \alpha \neq n\pi \\ \delta(u-t) & \alpha = 2n\pi \\ \delta(u+t) & \alpha = (2n \pm 1)\pi \end{cases} \quad (7)$$

where

$$A_\alpha = \sqrt{\frac{1 - j \cot \alpha}{2\pi}} \quad (8)$$

The inverse FRFT can be expressed as

$$x(t) = F^{-p}[X_p(u)] = \int_{-\infty}^{+\infty} X_p(u) K_{-p}(u, t) du \quad (9)$$

Equation (9) indicates that $x(t)$ can be represented by a set of orthogonal basis function $K_{-p}(t, u)$, whose weight coefficient is $X_p(u)$.

In practical applications, it needs adopt discrete FRFT as processing method, so in this paper, we choose an improved type of DFRFT proposed by Ozaktas [8].

IDFRFT & DFRFT

We rewrite the equation in equation (7)

$$t^2 \cot \alpha - 2tu \csc \alpha + u^2 \cot \alpha = t^2 (\cot \alpha - \csc \alpha) + (t-u)^2 \csc \alpha + u^2 (\cot \alpha - \csc \alpha) \quad (10)$$

when $\cot \alpha - \csc \alpha = -\tan(\alpha/2)$, equation (6) can be expressed as

$$\begin{aligned} X_p(u) &= A_\alpha \exp[j\pi(\cot \alpha - \csc \alpha)u^2] \cdot \int_{-\infty}^{+\infty} \exp[j\pi \csc \alpha(u-t)^2] \{ \exp[j\pi(\cot \alpha - \csc \alpha)t^2] x(t) \} dt \\ &= A_\alpha \exp[-j\pi \tan(\alpha/2)u^2] \cdot \int_{-\infty}^{+\infty} \exp[j\pi \csc \alpha(u-t)^2] \{ \exp[-j\pi \tan(\alpha/2)t^2] x(t) \} dt \end{aligned} \quad (11)$$

when $E_r(x) = \exp(j\pi x^2)$, r being $m = -\tan(\alpha/2)$ or $n = \csc \alpha$ equation (11) can be simplified as

$$X_p(u) = A_\alpha E_m(u) \int_{-\infty}^{+\infty} E_n(u-t) [E_m(t)x(t)] dt \quad (12)$$

2.3 The FRFT-based OFDM-LFM system

Figure 1 illustrates block diagram of the FRFT-based OFDM-LFM system.

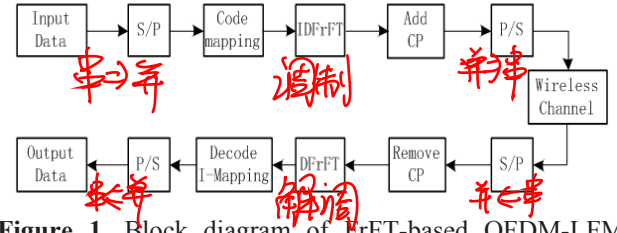


Figure 1. Block diagram of FrFT-based OFDM-LFM system.

2.4 Spectrum of Waveform

Through the Fourier transformation of $s(t)$

$$\begin{aligned} \tilde{S}(f) &= \int_{-\infty}^{+\infty} \sum_{m=1}^M \sum_{n=1}^N a_{n,m} \exp(j2\pi f_n t + j\pi \mu t^2) \cdot \text{rect}\left[\frac{t-(m-1)T}{T}\right] \exp(-j2\pi f t) dt \\ &= \sum_{m=1}^M \sum_{n=1}^N \int_{(m-1)T}^{mT} a_{n,m} \exp(j2\pi f_n t + j\pi \mu t^2) \cdot \exp(-j2\pi f t) dt \\ &= \sum_{m=1}^M \sum_{n=1}^N \int_{(m-1)T}^{mT} a_{n,m} \exp(j\pi \mu t^2) \cdot \exp[-j2\pi(f - f_n)t] dt \end{aligned} \quad (13)$$

when $\mu' = \pi\mu = \pi B/T$, $z = \sqrt{\frac{2}{\pi}} [\sqrt{\mu'} t - \frac{\pi(f - f_n)}{\sqrt{\mu'}}]$, then

equation (13) can be expressed as [9]

$$\tilde{S}(f) = \sum_{m=1}^M \sum_{n=1}^N \sqrt{\frac{\pi}{2\mu'}} \exp\left\{ \frac{-j\pi(f - f_n)^2}{\mu'} \right\} \int_{-z_1}^{z_2} \exp\left(\frac{j\pi z^2}{2} \right) dz \quad (14)$$

where

$$z_1 = \sqrt{\frac{2\mu'}{\pi}} \left(\frac{T}{2} + \frac{\pi(f - f_n)}{\mu'} \right) = \sqrt{\frac{BT}{2}} \left(1 + \frac{f - f_n}{B/2} \right) \quad (15)$$

$$z_2 = \sqrt{\frac{2\mu'}{\pi}} \left(\frac{T}{2} - \frac{\pi(f - f_n)}{\mu'} \right) = \sqrt{\frac{BT}{2}} \left(1 - \frac{f - f_n}{B/2} \right) \quad (16)$$

The Fresnel integrals, denoted by $C(z)$ and $S(z)$, are defined by

$$C(z) = \int_0^z \cos\left(\frac{\pi v^2}{2}\right) dv \quad (17)$$

$$S(z) = \int_0^z \sin\left(\frac{\pi v^2}{2}\right) dv \quad (18)$$

Fresnel integrals can be approximated by

$$C(z) \approx \frac{1}{2} + \frac{1}{\pi z} \sin\left(\frac{\pi}{2} z^2\right) \quad z \gg 1 \quad (19)$$

$$S(z) \approx \frac{1}{2} - \frac{1}{\pi z} \cos\left(\frac{\pi}{2} z^2\right) \quad z \gg 1 \quad (20)$$

Combining equation (19) with (20) into (14) and performing the integration yield

$$\tilde{S}(f) = \sum_{n=1}^{N_s} \left[\frac{\pi}{2\mu} \exp\left\{ \frac{-j\pi(f-f_n)^2}{\mu} \right\} \sum_{m=1}^M \{ [C(z_2) + C(z_1)] + j[S(z_2) + S(z_1)] \} \right] \quad (21)$$

Assume the OFDM-LFM symbol period $T = 1\mu s$, the number of symbols modulated on each subcarrier $M = 15$, the number of subcarriers $N = 50$, bandwidth of each LFM subcarrier $B_s = 1MHz$, Figure 2 shows the normalized frequency spectrum of OFDM-LFM waveform. It has an excellent spectrum characteristic similar to OFDM and the total bandwidth is consistent with equation (5).

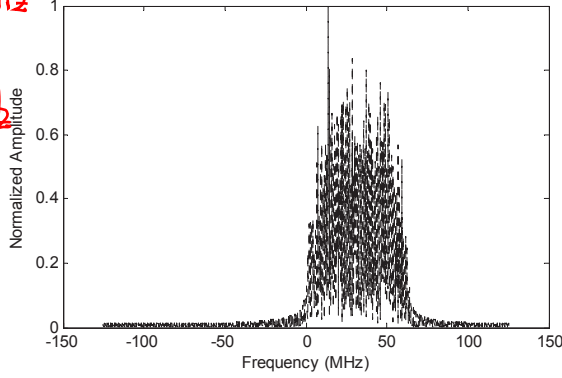


Figure 2. Normalized frequency spectrum of OFDM-LFM waveform.

3 Ambiguity Function Analysis

The ambiguity function of the OFDM-LFM waveform is

$$\begin{aligned} \chi(\tau, f_d) &= \int_{-\infty}^{+\infty} s(t)s^*(t-\tau) \exp(j2\pi f_d t) dt \\ &= \frac{1}{T} \cdot \exp[j2\pi(f_n \tau - \frac{1}{2} \mu \tau^2)] \int_{-\infty}^{+\infty} \exp[j2\pi(\beta + f_d)t] dt \quad (22) \\ &= \frac{c}{T} \int_{-\infty}^{+\infty} \exp(j2\pi \alpha t) dt \end{aligned}$$

where

$$c = \exp[j2\pi(f_n \tau - \frac{1}{2} \mu \tau^2)] \quad (23)$$

$$\alpha = \mu \tau + f_d \quad (24)$$

$$\beta = \mu \tau \quad (25)$$

Equation (22) can be expressed by simplifying

$$\chi(\tau, f_d) = \begin{cases} c \exp[j\pi \alpha (T - |\tau|)] \frac{\sin \pi \alpha (T - |\tau|)}{\pi \alpha (T - |\tau|)} \cdot \frac{(T - |\tau|)}{T}, & |\tau| \leq T \\ 0, & \text{else} \end{cases} \quad (26)$$

Considering the zero Doppler slice of the ambiguity function, namely, set $f_d = 0$. Equation (26) can develop into

$$|\chi(\tau, 0)| = c \cdot \exp[j\pi \mu \tau (T + \tau)] \cdot \left| \frac{\sin \pi \beta (T - |\tau|)}{\pi \beta (T - |\tau|)} \right| \cdot \left| \frac{T - |\tau|}{T} \right| \quad (27)$$

Also considering the zero delay slice of the ambiguity function, set $\tau = 0$, then get

$$|\chi(0, f_d)| = \left| \exp(j\pi f_d T_c) \frac{\sin \pi f_d T_c}{\pi f_d T_c} \right| \quad (28)$$

4 Simulation and Analysis

4.1 Ambiguity Function Simulation and Analysis

1) Comparing with OFDM radar-communication signal

Set the OFDM-LFM symbol period $T = 1\mu s$, the number of symbols modulated on each subcarrier $M = 15$, the number of subcarriers $N = 50$, bandwidth of each LFM subcarrier $B_s = 1MHz$. Figure 3 and Figure 4 illustrate diagrams of ambiguity function of OFDM and OFDM-LFM integrated radar-communication signal respectively.

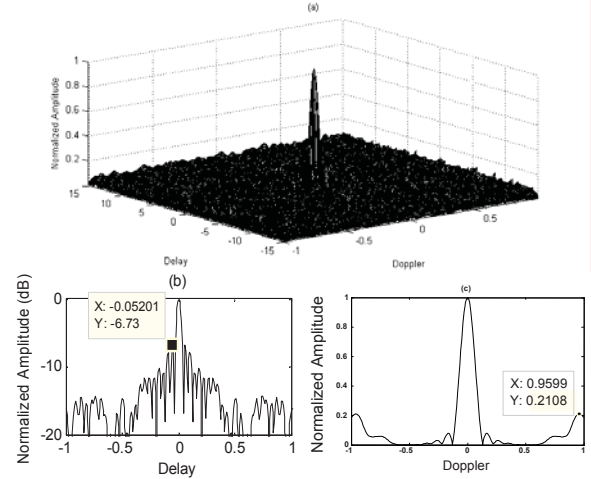


Figure 3. AF of OFDM radar-communication signal (a) 3D AF (b) zero Doppler slice (c) zero delay slice.

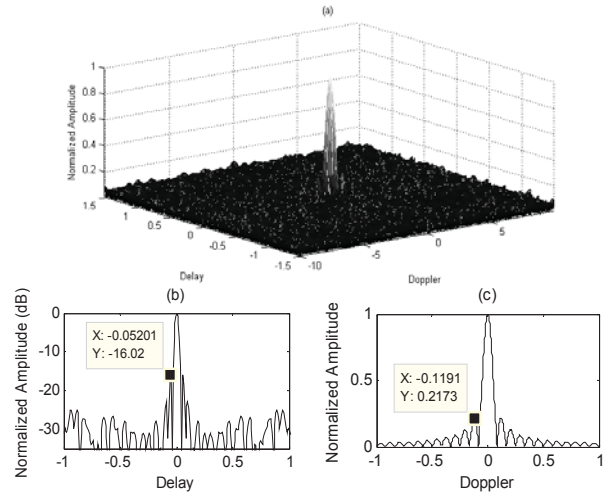


Figure 4. AF of OFDM-LFM radar-communication signal

(a) 3D AF (b) zero Doppler slice (c) zero delay slice.

Comparing Figure 3 and Figure 4 indicates that both ambiguity functions are all close to thumbtack shape, and OFDM-LFM has a narrower main-lobe and smaller side-lobe than OFDM, hence OFDM-LFM has a better delay resolution, and its Doppler resolution does not be affected.

2) Impact of LFM Coefficient

Set $T = 1\mu s$, $M = 15$, $N = 50$, Figure 5 and Figure 6 show OFDM-LFM ambiguity functions of different LFM coefficient.

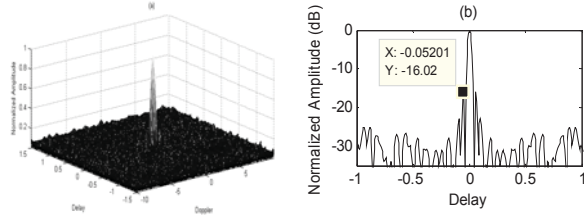


Figure 5. AF of $\mu = 1\text{MHz} / \mu_s$: (a) 3D AF (b) zero Doppler slice.

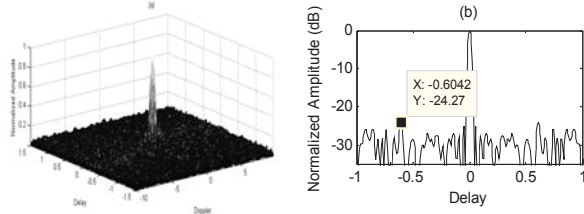


Figure 6. AF of $\mu = 2\text{MHz} / \mu_s$: (a) 3D AF (b) zero Doppler slice.

Figure 5 and Figure 6 indicate that the larger the LFM coefficient, the narrower main-lobe and smaller side-lobe are, that is, the better delay resolution.

3) Impact of Symbol Number

Set $T = 1\mu s$, $N = 50$, $B_s = 1\text{MHz}$, Figure 7 and Figure 8 show ambiguity functions of different symbol number.

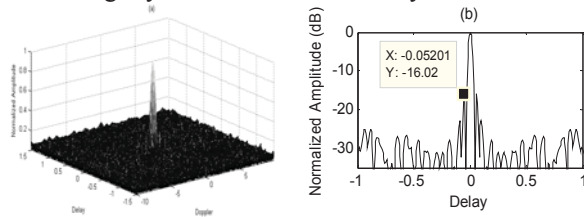


Figure 7. AF of $M = 15$: (a) 3D AF (b) zero Doppler slice.

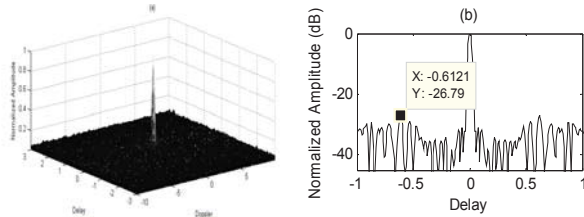


Figure 8. AF of $M = 30$: (a) 3D AF (b) zero Doppler slice.

μ 不变, $T_{\text{total}} = MT$;
 $B_s = MT_{\text{total}} = \mu MT \propto M$
 M 由 15 \rightarrow 30; B_s 由 15MHz \rightarrow 30MHz

From Figure 7 and Figure 8, we can see that the larger the number of symbols, the closer to thumbtack the ambiguity function, also, the smaller side-lobes of zero Doppler slice.

4) Impact of subcarrier number

Set $T = 1\mu s$, $M = 15$, $B_s = 1\text{MHz}$, Figure 9 and Figure 10 show ambiguity functions of different subcarrier number.

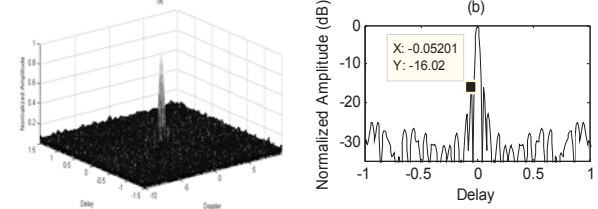


Figure 9. AF of $N = 50$: (a) 3D AF (b) zero Doppler slice.

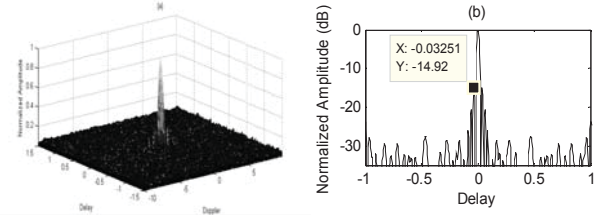


Figure 10. AF of $N = 80$: (a) 3D AF (b) zero Doppler slice.

Comparing Figure 9 with Figure 10, it can be discovered that the larger the subcarrier number, the narrower the main-lobe of zero Doppler slice, however, the side-lobes rise up slightly. Since subcarrier frequency interval decreases as the number of LFM subcarrier increases, it has led to serious coupling, and aggravated the performance of range resolution.

4.2 System Performance Analysis

1) Communication Performance

For the analysis of communication performance, we mainly calculate and analyze BER and throughput rate. Assume the simulation parameters are: the number of subcarriers $N = 52$, including the number of data subcarriers $N_{SD} = 48$ and the number of pilot subcarriers $N_{SP} = 4$; the sampling frequency is 20MHz; the symbol period $T = 1\mu s$, including cyclic prefix $CP = 200ns$ and FRFT or FFT period $TF = 800ns$; the frequency interval $\Delta f = 1.25\text{MHz}$; the modulation is 16-QAM. We also assume the communication link between two platforms is the Line-Of-Sight (LOS) single-path, and adopt ideal channel and Rayleigh channel with 100Hz maximum Doppler shift for evaluating. Figure 11 shows BER of OFDM-LFM system based on FRFT, comparing with OFDM system based on FFT.

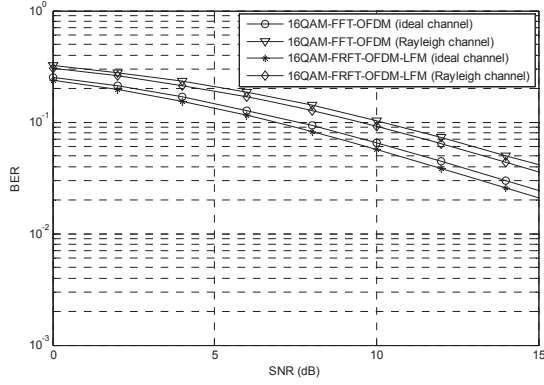


Figure 11. BER performance of FRFT-based OFDM-LFM compared to the FT-based OFDM in ideal and Rayleigh channel.

Figure 11 indicates that BER performance evaluated through Rayleigh channel decreases when comparing with that in an ideal channel, and there is an improvement in the performance of OFDM-LFM system based on FRFT compared to the OFDM system.

Then, consider the platform rotates clock-wise, the other rotates anticlockwise when they are communicating with each other. Assume the radar antenna beam angle directs to 0° , pitch beam directing is 10° , main beam antenna maximum gain is 20dB , antenna minimum gain is -20dB , antenna beam width is 3° , average transmitted power is 100W , power loss in the antenna is 0.5 , receiver noise figure is 4dB , and the distance between two platforms is 5km . Then, we can get a Probability Density Function (PDF) diagram of throughput rate illustrated in Figure 12.

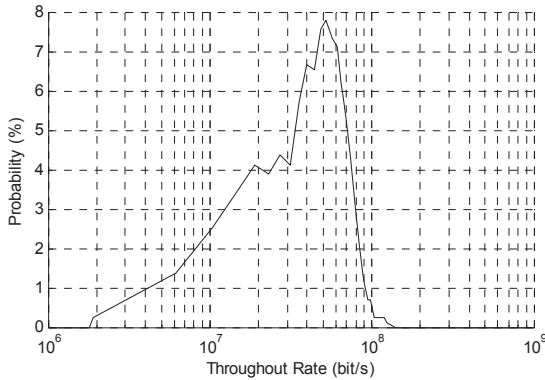


Figure 12. Throughput rate performance of OFDM-LFM.

From the curve exhibited clearly in Figure 12, we can calculate the average throughput rate in communication link is approximately 49.541Mbps . So the communication transmission rate of OFDM-LFM system based on FRFT can satisfy the need for transmitting large number of data.

2) Radar Performance

For the analysis of radar performance in OFDM-LFM system based on FRFT. Consider making a simulation experiment between two adjacent target range profiles, assuming bandwidth of each subcarrier $B_s = 1\text{MHz}$, the

number of subcarriers $N = 50$, transmitted frequency $f_0 = 10\text{GHz}$. Set the initial position of range profile is 1km , the distances between targets and platform are 1.1km and 1.103km , radar cross section is 1m^2 , target velocity is 0m/s with respect to platform, the result is shown in Figure 13.

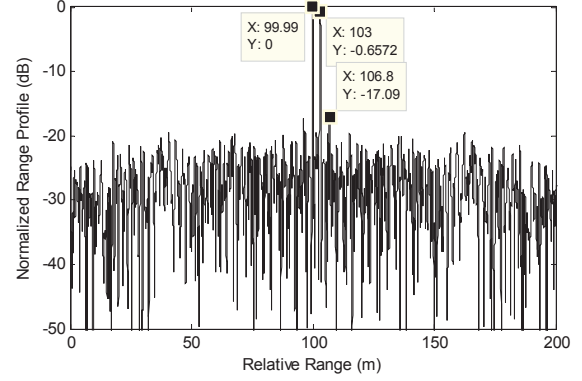


Figure 13. Range Profile of two adjacent targets.

Figure 13 indicates that there are two obvious peaks of targets at 1.1km and 1.103km , and the peak of main-lobe is narrow and maximum side-lobe besides main-lobe being -17.09dB , thus, OFDM-LFM integrated signal with bandwidth of 50MHz can distinguish two targets 3m apart distinctly, moreover, it can obtain a better range resolution compared with theoretical value.

Conclusions

In this work, we have presented a novel integrated radar-communication signal of OFDM-LFM, which uses orthogonal LFM signals as subcarriers and uses FRFT as modulation and demodulation method. For the aspects of spectrum distribution and factors on radar ambiguity function, we have made a thorough analysis, and take a further research on communication and radar performance afterwards. Simulation results shows that our integrated signal can obtain a better performance of range resolution, further more it is more suitable for the frequency-selective channel than the traditional OFDM integrated signal and can satisfy the demand of transmitting a large number of data.

Acknowledgments

This work was supported by the National Natural Science Foundation of China (No. 61301155). Thanks are due to Prof. Wei Zhang for assistance with the guidance and to Yang Liu for valuable discussion.

References

- [1] Li Tingjun, Ren Jiancun, Zhao Yuanli, Zhang Jinhua, "Research of Radar-Communication Integration", Modern Radar, 2001.
- [2] Robertson, M., Brown, E.R., "Integrated Radar and Communication based on Chirp Spread-Spectrum

- Techniques”, IEEE MTT-S Int. Microwave Symposium, Philadelphia, USA, 2003, pp. 611–614.
- [3] Li Xiaobo, Yang Ruijuan, Chen Xinyong, Cheng Wei, “The Sharing Signal for Integrated Radar and Communication Based on FRFT”, SIGNAL PROCESSING, 2012, 28, (4), pp.487-494.
 - [4] Donnet, B.J., Longstaff, I.D., “Combining MIMO radar with OFDM communication”, 3rd European Radar Conference, 2006, pp. 37-40.
 - [5] Sturm, C., Zwick, T., Wiesbeck, W., “An OFDM system concept for joint radar and communications operations”, IEEE 69th Vehicular Technology Conference, Barcelona, 2009, pp. 1-5.
 - [6] Cheng Fang, He Zishu, Liu Hongming, Li Jun, “The Parameter Setting Problem of Signal OFDM-LFM for MIMO Radar”, International Conference on Communications Circuits and System (ICCCAS), 2008, pp. 876-880.
 - [7] Tao Ran, Qi Lin, Wang Yue, “Theory and Applications of the Fractional Fourier Transform”. Beijing: Tsinghua Univ. Press, 2004.
 - [8] Ozaktas, H.M., Arikan, O., et al. “Digital Computation of the Fractional Fourier Transform”, IEEE Trans. Signal Processing, 1996, 44, (9), pp. 2141-2150.
 - [9] Bassem, R., Mahafza, “Radar Signal Analysis and processing using MATLAB”, New York: Chapman&Hall, 2009, pp. 109-114.